CAPSTONE PROJECT II 4TR3: FINAL REPORT WINTER 2020

Creating a Python based automated image analysis tool for Atomic Force Microscopic (AFM) images: Important parameters for making a high sensitivity localized surface plasmon resonance (LSPR) based sensor and its possible application in the creation of a quality control tool

---

Nikhil Saini (400047123)
Supervisor: Dr.Fei Geng and Dr.Ayse Turak
December 12, 2020

Acknowledgement

I would first like to express our sincerest gratitude to Dr. Ayse Turak, professor at the School of Engineering Physics and supervisor of this research project at McMaster University. Dr. Turak has provided us with all the required support for the smooth transition of the project throughout, it would have not been possible without her guidance and support. Dr. Turak, your generosity is greatly appreciated. Your validations have always given me the motivation to move forward with my decisions.

I would also like to thank Dr. Fei Geng for timely guidance, understanding, support and motivation during this tough COVID-19 pandemic times. I would also like to thank Dr. Geng for always helping and supporting me in the decision-making process.

Lastly, I would like to thank Ramis Arbi and Munir Mohammad PhD students in the Turak Lab for providing me with all the required data and helping me with brain storming. This report's Acknowledgment, Abstract, Introduction, Materials Methods, Results, Discussion, References, and required literature review is written by Nikhil Saini.

TABLE OF CONTENTS

1. Abstract

This project focuses on creating a Python based automated image analysis tool for atomic force microscopy (AFM) images of nanoparticles coated on a substrate. This program can provide one with detailed information about the surface morphology of the fabricated layer including, particle count, the approximate centre coordinate of the particles, an approximate radius, and its height distribution. The efficiency of this tool was measured by using atomic force microscopy (AFM) images obtained from members of Turak lab. Additionally, in this work members of Turak lab created gold nanoparticles through different synthesis approaches and also used different deposition techniques to coat these Au NPs on glass substrate in attempt to make localized surface plasmon resonance (LSPR) based sensor. Different approaches were tried in order to see which one is most suitable for fabricating LSPR sensor. In order to determine the most affective synthesis and deposition approaches they collected UV-Vis absorbance spectrum and AFM images of each surface. From the provided UV-Vis data, it was concluded that out of all the applied approaches, both APTES ((3-Aminopropyl)triethoxysilane) based adhesion techniques were the most effective in creating LSPR sensor chips. This is because by using this technique, one of the important LSPR parameters, the thickness of the coated layer, can be easily tuned by changing the immersion time and size of Au NPs. The UV-Vis data of the chips fabricated using the APTES based approaches, in which plane glass was immersed in a mixture of APTES and Au NP aqueous solution, provided us with an optimal layer thickness with 25% - 30% light absorbing ability after 15 hours of immersion time. Using this approach, the thickness can be tuned by changing the immersion time. Other APTES based approaches, in which glass was first functionalized with APTES molecules then immersed into Au NP solution, did not provide us with an optimal thickness with 25% - 30% light absorbing ability. However, we observed an increase in thickness after using Au NPs of greater size. Thus, this approach is size dependent and by using this approach, we can achieve the optimal thickness with 25% - 30% light absorbing ability by increasing the size of Au NPs. These are promising approaches but still needs to be further optimized to achieve Au NPs with a narrow size distribution to accomplish narrower UV-Vis absorption spectrums and a sensor with better sensitivity. After all the optimizations, a standard Au NP synthesis and deposition approach will be established which could be used to fabricate an LSPR sensor of desired surface morphology and absorption spectrum, which could be observed under AFM and UV-Vis respectively. Thereupon, this finalized data could be used with the Python based image analysis tool and utilized as a quality control tool for sensor chips fabricated using the standardized protocol.

2. Introduction

Nanoparticles are a cluster of molecules that form particles ranging from 1-100 nm. Gold nanoparticles exhibit different optical properties with changing size. Gold nanoparticles strongly absorb light at around 520 nm to 650 nm and a surface plasmon effect is also observed at this wavelength. Gold is a conducting material which means it has electrons which can be energized and excited so they can travel freely in the material. When there is no energy provided, these electrons are at a lower energy level (valance band) and as these electrons are provided with sufficient energy, they jump into a conduction band; these electrons at higher energy levels are called conduction band electrons (Ghosh et al.).

When the incident electromagnetic field comes in contact with nanoparticles, it causes the conduction band electrons to undergo coherent oscillation which causes the formation of an electromagnetic field which can propagate between the conducting metal and dielectric (glass) at different frequencies. When the oscillation mode from an electromagnetic field (light) is coupled to the oscillation of conducting electrons, then resonating electrons are called surface plasmons. An absorption band is observed when the incident photon frequency is in resonance with the collective oscillation of the conduction band electron and this phenomenon is known as surface plasmon resonance. This property is used to study different protein interactions by monitoring the slight shifts in absorbance. Metallic nanoparticles such as gold, silver, aluminium and platinum, are well known to show localized surface plasmon resonance (LSPR), but gold is most popular because of its ability to stay in its noble form. (Ghosh et al.)

The resonating frequency of the gold changes with size, shape, inter-particle interactions, dielectric properties, and the local environment of the nanoparticle (Nicoya et al.). The electron's oscillation is highly dependent on the density of electrons, the effective electron mass, the shape, and the size of the charge distribution. The sensitivity of LSPR based instruments can be tuned by changing all these parameters as per the requirement. Gold nanoparticles exhibit different optical properties with change in their size and distribution over a surface. The absorbance changes with clustering because of more red light being absorbed. With small size particles, the absorbance shifts towards pink/violet light (Ghosh et al). The LSPR sensing technique is based on real time measurements of slight shifts in reference absorbance peak as a function of absorbed (forward shift) and desorbed (backward shift) material on the sensor surface. As the material is absorbed on the surface, the absorbance peak shifts towards blue spectra, and as the material is desorbed, the absorbance peak shifts towards red spectra (Figure 2.1) (Nicoya et al.).

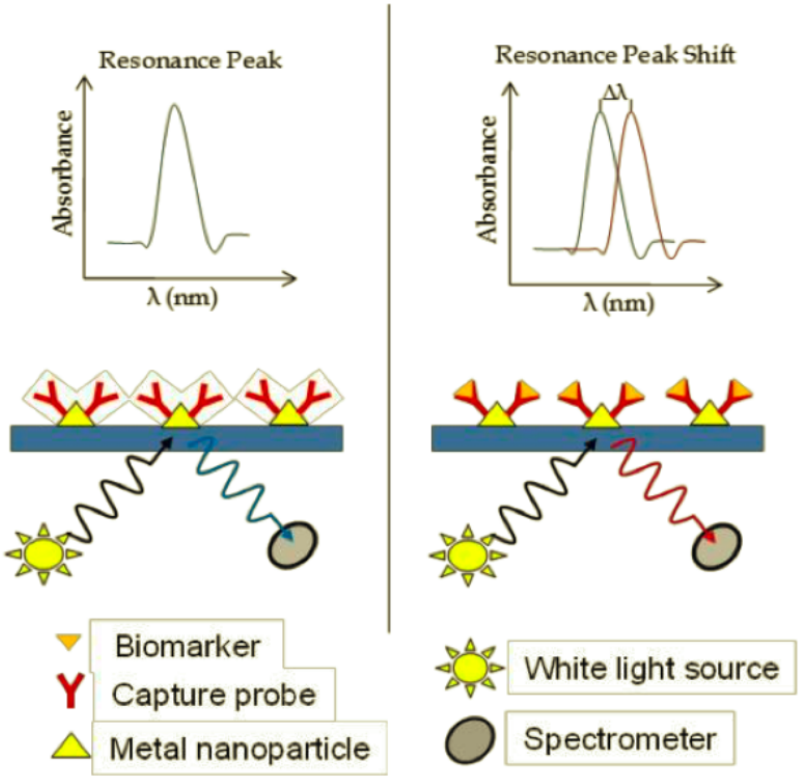

Figure 2.1 - Illustration of LSPR sensing

We focused on the use of localized surface plasmon resonance (LSPR) phenomenon in different bimolecular detection and in other upcoming sensing technologies. In order to utilize this phenomenon in sensing technologies, uniformly sized gold nanoparticles are coated on a glass surface in different patterns. The sensitivity of the surface is dependent on different parameters including size, shape, uniformity, and thickness of the layer. Sensitivity and performance of the LSPR sensor can be monitored by the following equations, Equation 1 and Equation 2 (Nicoya et al.):

$$R = m\Delta n(1 - e^{\frac{-2d}{l_d}})$$

Equation 1

Where 'R' is the sensor response to absorbed layer on the sensor, 'm' is refractive index sensitivity, 'n' is the difference in refractive index between absorbed layer and surrounding medium, 'ld' is electromagnetic decay length and 'd' is the thickness of the absorbed layer on the sensor. This equation can be derived by analysis of data obtained by observing the

shift in absorbance peak with the changing thickness of the absorbed material on surface. An example of deriving such an equation from LSPR response is shown in figure 2.2. In this example, a slight shift in reference absorbance peak is observed with changing the thickness of the absorbed layer. Sensor surface is absorbed with polyelectrolytes of different lengths to create layers of varying thickness. Later, the relationship between the sensor response and thickness is derived by plotting the shift in the LSPR peak against the layer thickness.

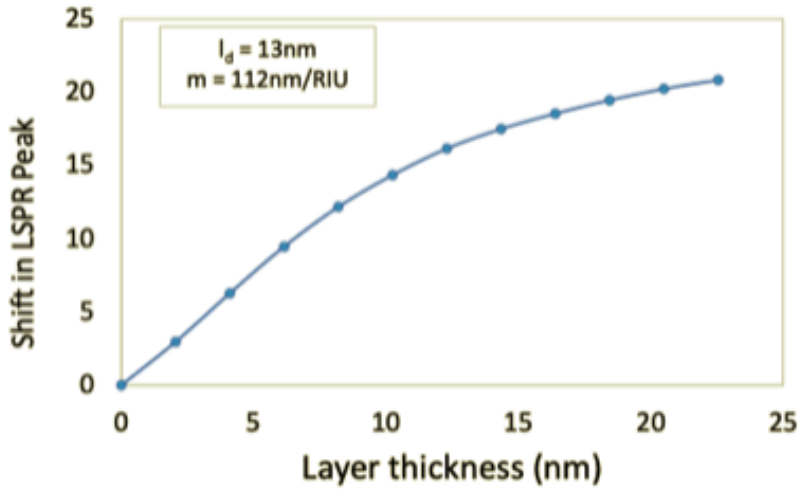

Figure 2.2 - Experimental data of LSPR peak shift with changing thickness of absorbed polyelectrolyte on gold nanoparticle surface

Another essential parameter to determine the sensitivity of the sensor is the figure of merit (FOM) which can be calculated as shown in equation-2.

$$FOM = \frac{m}{\Delta\lambda}$$

Equation 2

Where '' is the width of half the maximum of the LSPR absorbance peak. The higher the 'm' value and the smaller the width will give a higher FOM, thus a higher sensitivity sensor. The smaller width of the half maximum can be achieved by using a nanoparticle solution which has narrow size distribution of nanoparticles in it.

The aforementioned approach can be used for measuring the sensitivity of the LSPR sensor surface and for establishing the standardized sensor fabrication protocol. After optimization, this protocol will help us in producing sensor chips with specific surface morphology.

After determining the standard fabrication procedure which would provide us with sensor of desired sensitivity and specific surface morphology. This morphological data of desired sensor can be used to further model this Python program to distinguish between a good and bad sensor, hence, this would work as a quality control tool for our fabrication procedure.

There have been different sensor developments for monitoring the pH, DNA detection and protein interactions using the LSPR response. Tokareva et al., Ruhe et al., Biesalski et al., Houbenov et al. and Guo et al. have demonstrated the process of making real time monitoring of swelling and shrinking of responsive ultrathin polymer brushes using SPR sensing technology. 4nm gold coated substrate was modified with three layers PGMA, P2VP and gold nanoparticles. They used different polyelectrolyte to make a brush like structure (Figure 2.3). Poly-electrolytes have different change density in their interior regions with changing pH of their environment. This causes electrostatic repulsion causing stretching and shrinking of the polymer brush. This phenomenon causes changes in the electron density over the surface which results in changes in the SPR response. This is used as an indicator for pH, and change is monitored by measuring absorbance.

In Tokareva et al. paper, they used gold nano-islands formed on a glass slide using vapour deposition as a substrate to measure the SPR signal. They performed vapour deposition of gold as mentioned in Iyer et al. paper. A gold coated glass slide was coated with three different layers to make the real time monitoring system for swelling and shrinking. Gold islands were coated with polyglycidyl methacrylate (PGMA) followed by poly(2vinylpyridine) (P2VP) polymer brushes and a layer of gold (Figure 2.3). The absorption varied with a shift of 6 nm between pH 2 and pH 5. As the pH reduces, the polyelectrolyte brushes get more protonated (positively charged) which causes electrostatic repulsion inside the chain causing it to swell. This application could be useful in monitoring ph in sensitive reactions or binding kinetics.

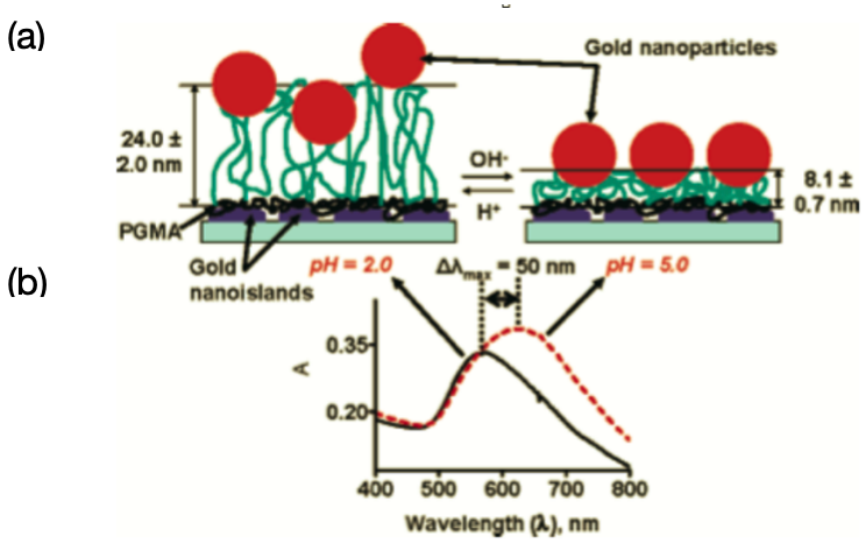

Figure 2.3 - (a): Schematics of the reversible pH change-induced swelling of gold nanoparticle- coated P2VP polymer brush. (b): T-SPR spectra of gold nano islands (containing absorbed PGMA, P2VP polymer brush, and Au NP) at pH 2 and 5 (Tokareva et al.)

Recent ongoing research in the Turak lab is the application of LSPR bio-sensing in leveraging the use of LSPR technology to make a rapid screening technology for validating any antiviral surface that has the potential to denature/deactivate the SARS-Cov-2 viral components which lead to infection. The basis of screening is highly dependent on the binding kinetics of human Angiotensin-converting enzyme 2 (ACE2) with SARS-Cov-2 S1 subunit glycoprotein protein. In this screening setup, ACE2 is immobilized in a LSPR bio-sensor surface and S1 is used as the analyte. We hypothesize that as the viral protein comes in contact with the antiviral surface, the surface will affect its glycosylation or denature the protein, hampering the ability of the virus to bind with ACE2, hence deactivating the virus. This change in the viral protein will reduce its ability to bind with immobilized ACE2 receptors on the LSPR biosensor, and this changing binding kinetics can be monitored using the SPR instrument. In order to validate the efficiency of the antiviral surface, members of Turak lab will establish the binding kinetics of the S1 protein with ACE-2 before and after incubating the S1 (viral protein) on the antiviral surface (Figure 2.4). The scalable reduction in binding kinetics between S1 with ACE2 after incubation on an antiviral surface will describe the efficiency of the antiviral surfaces and candidate materials.

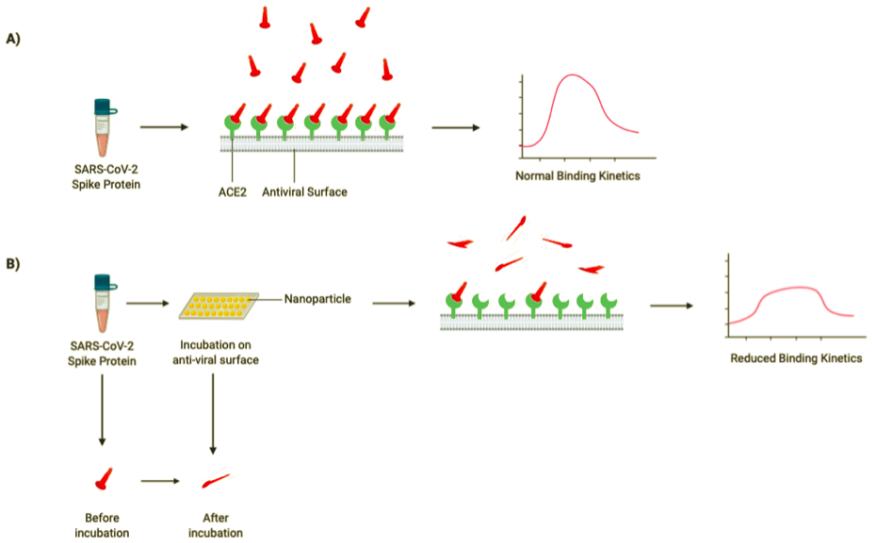

Figure 2.4 – SPR based rapid screening methodology for screening efficiency of different antiviral surfaces. (A) High binding kinetics of S1 spike protein with ACE2 before its exposure to engineered surface (B) Reduced binding kinetics of S1 spike protein with ACE2 after its exposure to engineered surface.

In the past, different LSPR sensor fabrication techniques have been evolved including adhesion techniques and vapour deposition techniques. In one of the examples for adhesion techniques, the glass was first covalently functionalized with APTES. Successful functionalization leads to formation of siloxane bonds between the silicone atom of APTES and hydroxide groups of glass and the primary amine group of the molecule will be facing outwards making the glass surface positively charged. This chip is immersed into citrate synthesized gold nanoparticles and left for 12 to 48 hours. During the incubation period, the negatively charged gold nanoparticles go under electrostatic adhesion with positively charged primary amine on the surface (Xie, L. Et al.). Vapour deposition approaches use a mask to achieve nano islands on the surface and such a technique is mostly used in making reflection based LSPR sensor chips (Shin YB et al.).

In an attempt to create the LSPR sensors, members of Turak lab used two different synthesis approaches to make Au NP which involve reverse micelle templated gold nanoparticles and reduction of gold salt in aqueous solution using trisodium citrate. Reverse micelle templated gold nanoparticles were deposited on the glass surface using spin coating and etched with argon for 20 mins, and aqueous solution based gold nanoparticles were coated onto glass surface using two different APTES based adhesion procedures. In first APTES based approach, the glass was first functionalized with APTES molecule and then Au NPs were adhered onto the surface by immersing the functionalized surface inside the Au NP solution for 24 hours. In this approach, two different functionalized glass substrates were

immersed into two different Au NP solutions, one with smaller nanoparticles and other one with bigger nanoparticles. In the second APTES based approach, three plane glass slide were immersed in a mixture of APTES and Au NP solution for different time intervals (15, 20, 24 hours). Absorbance spectrum of all the chips, prepared through different approaches, were compared with the absorbance spectrum of commercially available chip bought from Nicoya Life-science as a control.

Python based image analysis tool for AFM images is created to automate the image analysis procedure and to allow for a rapid way of analyzing AFM images of nanoparticles coated on a substrate. The program is able to determine the aforementioned details about the surface morphology. This program works in two steps. The first step involves creating a mask for the original image, and an overlap of the mask and original image (Figure 2.4). The mask and the overlap image is further used for calculating the following parameters:

1. Particle count
2. Centre coordinates
3. Approximate radius
4. Height distribution

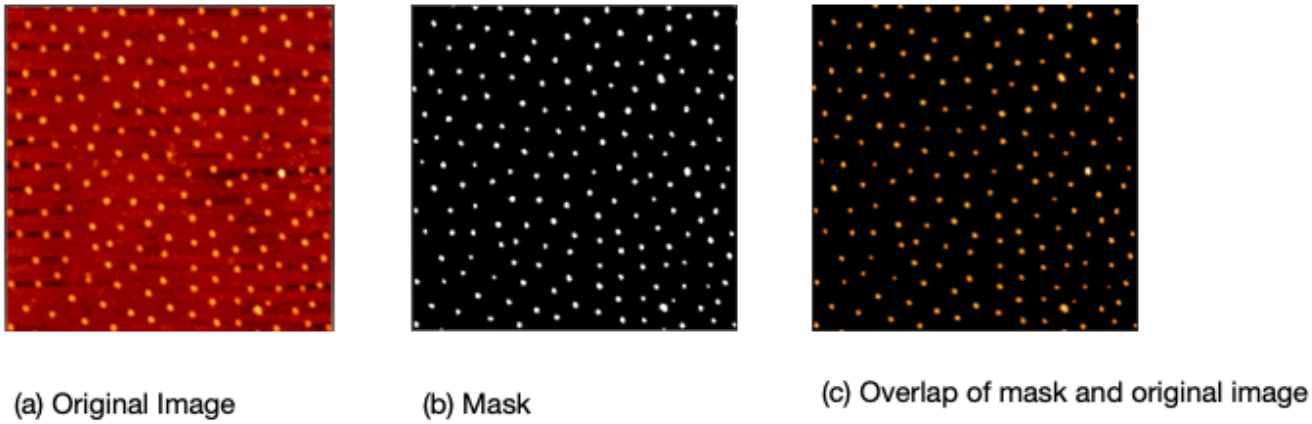

Figure 2.4 - Illustration of first step of Python based image analysis tool. The original image (a) is obtained from Turak lab and is used as a sample image to explain the working procedure of the software created (Image name - PYI_PbI_4824_et450001)

3. Materials and Methods

3.1 Data (Images and UV-Vis data)

Sample AFM images for testing Python program, AFM images of Au NP coated on glass and UV-Vis data obtained from Turak lab. Name of image used for testing this Python tool is PYI_PbI_4824_et450001 (Figure 2.4 (a))

3.2 Software requirements for running Python program

Python 3, python libraries - mpl_toolkits, matplotlib.pyplot, numpy, matplotlib.image, OpenCV2, seaborn, scipy, statistics, WSXM and Anaconda IDE for data visualization. All these softwares required for running this tool are available free of cost online.

3.3 Working description of each function of Python program

3.3.1 Creating mask of original image, and an overlap of mask and original image

In an AFM image extracted from WSXM, the heights are represented in form of a colour intensity. The brightest pixel in image is considered as the highest point and darkest pixel is considered as the lowest point. Before using this Python tool, WSXM software was used to extract data from a .ibw data file obtained from an AFM instrument and the image of interest was saved as in the .jpg format. Along with .jpg format of the image of interest, the same image should also be saved as ASCII file format. ASCII file is a text file which saves the image in form of three dimensional coordinate format. This file has X, Y, Z coordinates, where X and Y are the the location of each point scanned by AFM instrument, and Z is the height of that point in nanometers.

The first step allows you to separate the background from particles and distinguish each particle by creating a boundary around them. The unwanted background is converted into black colour leaving the particles behind (Figure 2.4 (c)). This separation makes it easy for the computer to distinguish between different contours present in the image and it can count the number of contours easily.

3.3.2 Particle counting and centre coordinates

The program uses the overlap image (Figure 2.4 (c)) and the couture finding function from the CV2 library to the count number of particles. Total number of contours is equal to the number of particles present in the image. After finding each contour, the software finds the brightest points in each contour and registers it as an approximate centre coordinate of the particle (Figure 3.1 - centre coordinate of each particle marked blue in middle of each particle). Each contour (particle) gives one coordinate. These coordinates are then utilized in the Dislocate software to create a visual description of packing/distribution of particles on surface.

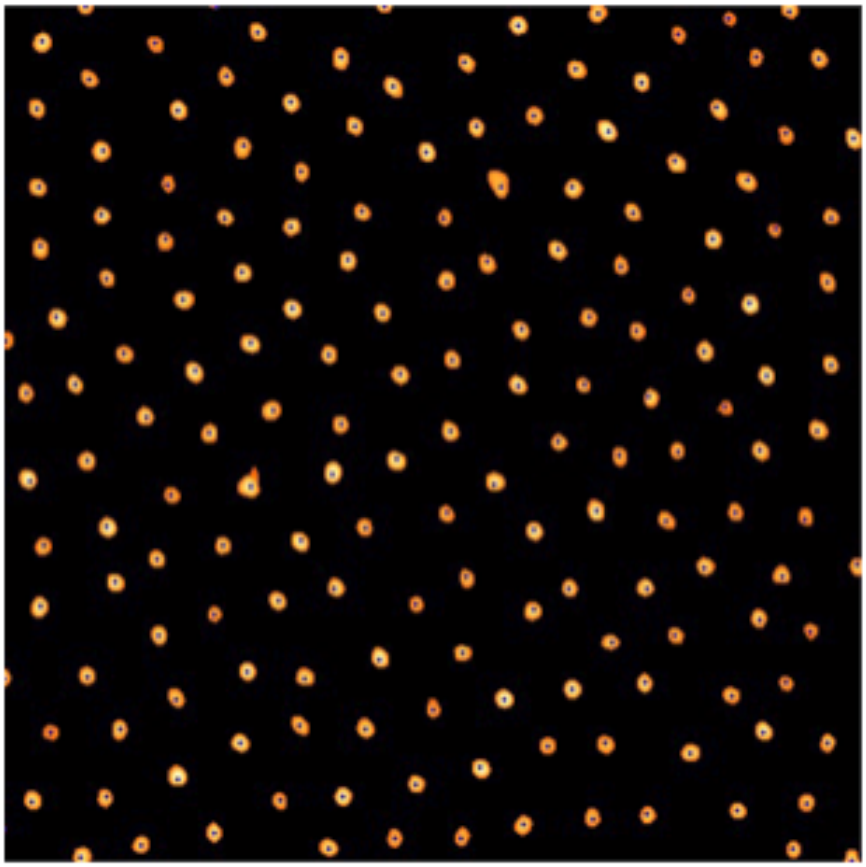

Figure 3.1 - centre coordinate of each particle marked blue in middle of each particle

3.3.3 Approximate radius

After finding the contours (particles), the software uses the CV2 library to find the biggest enclosing circle for each contour (Figure 3.2), and finds the radius of those biggest enclosing circles. These radii are considered as the approximate radius of each nanoparticle.

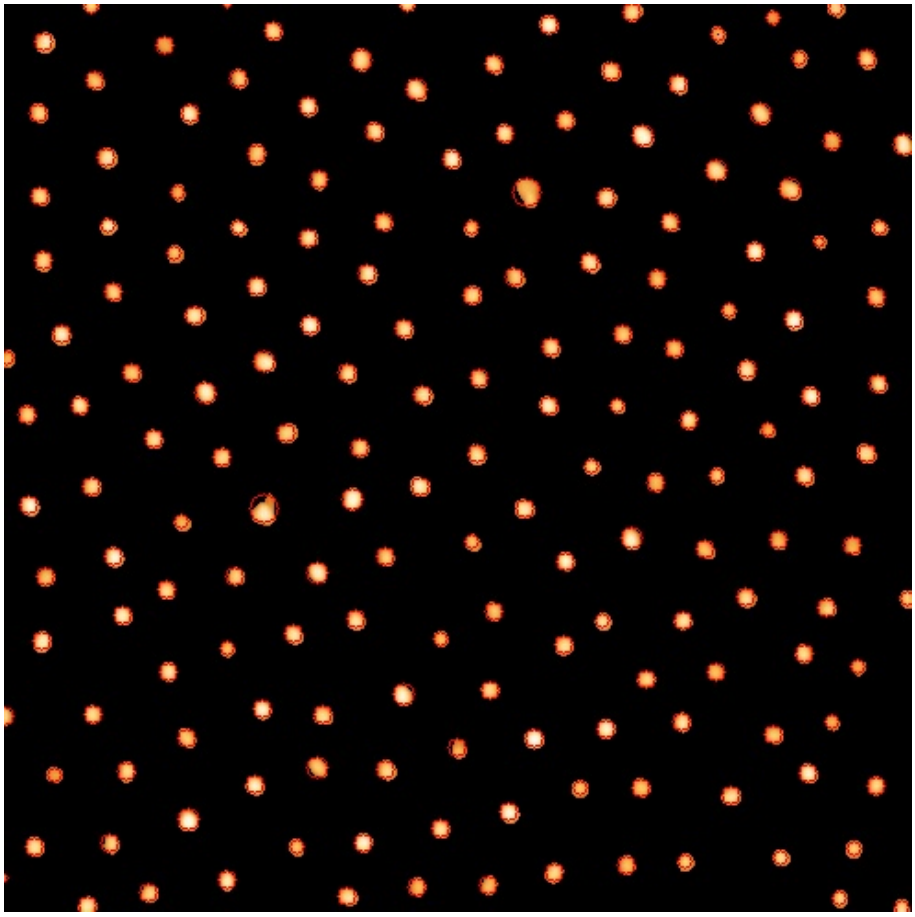

Figure 3.2 - Biggest enclosing circle for each contour (particle) marked in red

3.3.4 Height distribution

This part of the the software uses overlap image (Figure 2.4 (c)) to find the height distribution. Using the overlap image software finds the percent of black pixels (black pixels are considered as the background) and using this percentage, the software separates the background heights from nanoparticle heights from ASCII text file. The average background height is subtracted from all the heights that are considered as heights of nanoparticles. This subtracted height data is plotted on a histogram (Figure 3.3) showing the height distribution of nanoparticles on the surface.

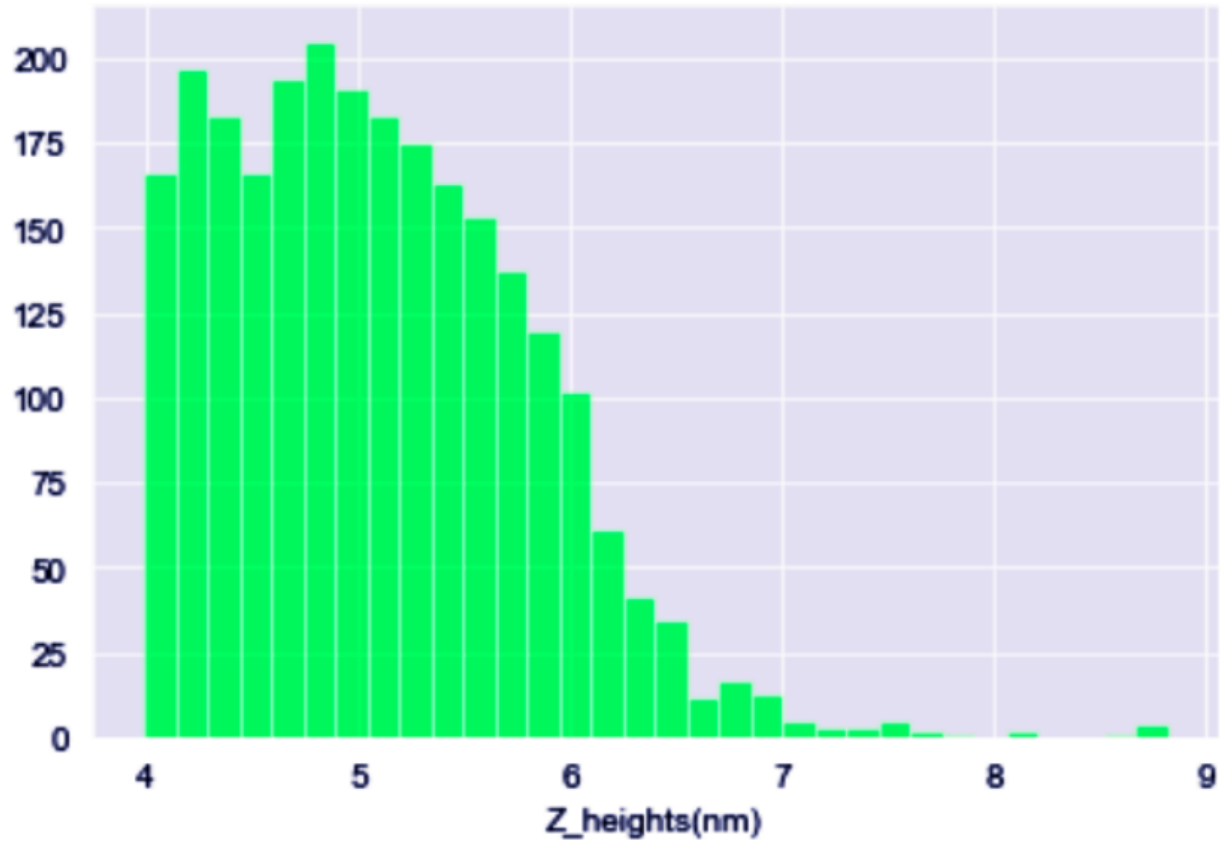

Figure 3.3 - Height distribution of figure 2.4(a) obtained from height distribution feature of the tool

3.4 UV-Vis data for approaches used for LSPR sensor surface preparation

The UV-Vis spectra for seven different samples were obtained from members of the Turak lab, where six of them were sensors created using different approaches and the seventh spectrum was of Nicoya's commercially available chip for comparison.

Table 1 - UV-Vis spectrums description and systematic arrangement of samples

Approaches	**Micelle templated**	**APTES Functionalization glass**	**Au NP solution + APTES solution mixture used on un-functionalized glass surface**	**Nicoya's chip**	**Total samples**
Approach description	Au NP synthesized using reverse micelle and deposited on surface using spin coating and etching with Argon for 20 mins	Glass is first functionalized with APTES and then immersed in different Au NP aqueous solutions for a time interval	Clean glass is immersed in mixture of APTES and Au NP aqueous solution for different time intervals	Commercially available LSPR sensor chip used for comparison	
Number of samples	One sample	Two samples - each sample is immersed in 2 different solutions with Au NP of different sizes each for 24 hours	Three samples - each sample is immersed in Au NP solution for different time intervals (15, 20, 24 hours)	One	Seven

4. Results

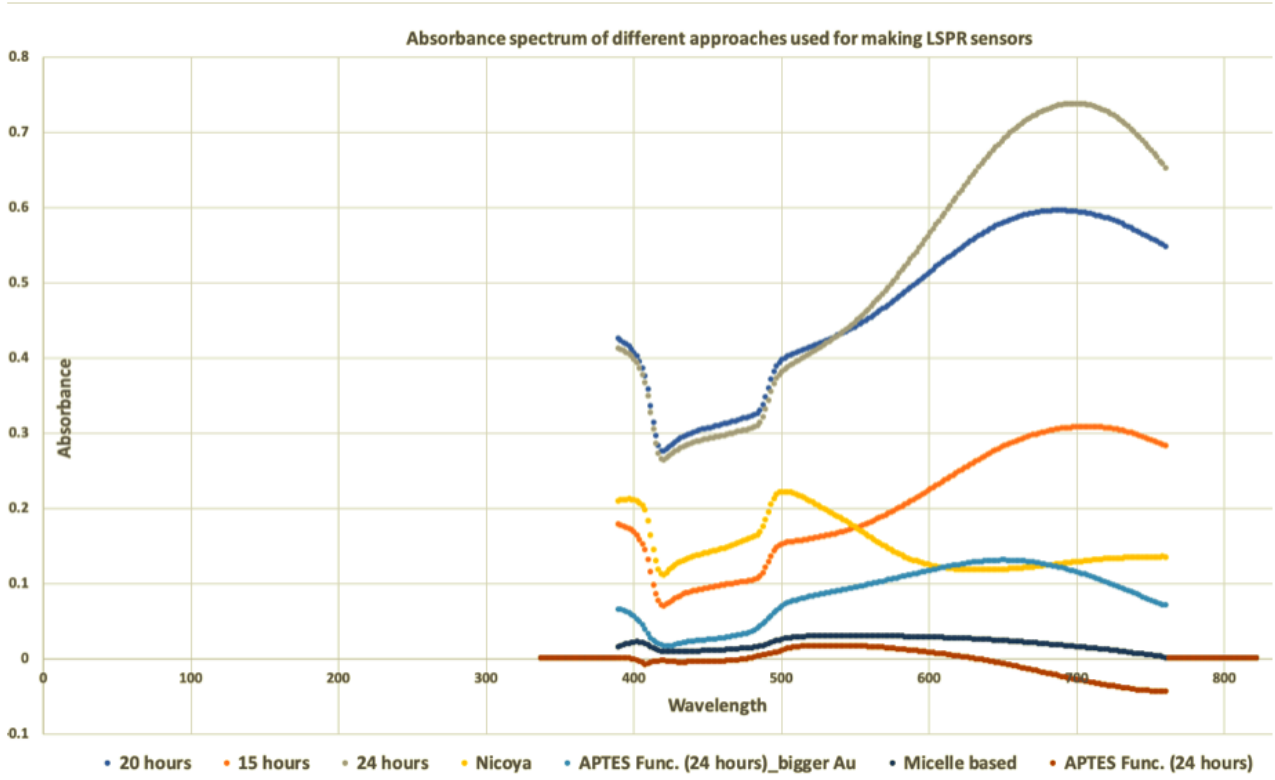

Figure 4.1 - UV-Vis absorbance spectrum of LSPR sensor surfaces fabricated using different approaches. Sample details:- (a) 20 hours, 15 hours, 24 hours - absorbance spectra of three different plain glass slides immersed in mixture of APTES and AuNP solution for those three different time intervals; (b) Nicoya - absorbance spectra of commercially available LSPR sensor chip from Nicoya life sciences; (c) APTES Func. (24 hour)_bigger Au - absorbance spectra of glass slide first functionalized with APTES molecules and then immersed in solution with greater AuNPs for 24 hours; (d) APTES Func. (24 hour) - absorbance spectra of glass slide first functionalized with APTES molecules and then immersed in AuNP solution with smaller particles as compared to solution used in sample (c) for 24 hours; (e) Micelle based - absorbance spectrum of chips fabricated by spin coating reverse micelle templated Au NPs and etched for 20 mins with Argon

The absorbance of the LSPR chips, fabricated using reverse micelle templated Au NPs, is around 2 % (Figure 4.1 (e)), which means that there is not enough material on surface and 99 % of light is getting transmitted. In comparison with absorbance (25 %) of the commercially

available LSPR chip from Nicoya (Figure 4.1 (b)), this fabrication has 23 % less absorbance. Amongst the sensor surfaces created by immersing the APTES functionalized glass in Au NP solution for 24 hours, the one immersed in solution with bigger particles has a higher absorption of 15 % (Figure 4.1 (c)) as compared to the one which was immersed in solution with smaller size particles (1% absorbance) (Figure 4.1 (d)). As per Figure 4.1 (a), it looks like that the fabricated chips, after immersing the plane glass in a mixture of APTES and Au NP for different time intervals, increased in absorption of light with increases in immersion time as well. Specifically, the absorption 15 hours, 20 hours and 24 hours was determined to be at 30 %, 50 % and 75 % respectively. The width of half maximum of all the absorbance peaks are very wide as compared to the Nicoya sensor chip which indicates that the size distribution of Au NPs on the surface is very broad.

5. Discussion

The aim of this project was to create a Python based image analysis tool for AFM images and we hypothesized how it could be further used as a quality control tool for fabricated LSPR sensors. We also analyzed the UV-Vis spectrum for different approaches attempted to create LSPR sensors and filtered out the techniques which could be successfully used in making sensors with high sensitivity in the future. From the results obtained, we found that two different APTES based approaches can be successfully used in the future to create the desired LSPR sensors with minimum absorbance of 25% and a narrow absorbance peak with a maximum width of 50 nm (standard from Nicoya's chip). As per Figure 4.1, it can be concluded that for the APTES based adhesion technique, in which glass slides are first functionalized with APTES molecules and then immersed in Au NP solution, with increasing particle size, there is an increase in absorbance value with increases in the Au NP size. Hence, in order to achieve the desired absorption (25% - 30%) and a narrow spectrum peak using this technique, we need to use Au NP solution with bigger nanoparticles. After immersing the functionalized surface with smaller Au NP solution for 24 hours, the absorption value was 1%, whereas when the functionalized glass was immersed in Au NP solution with bigger particles for 24 hours the absorbance value increased to 15 %. In this approach, the thickness or absorbance value did not change with increases in the immersion time, which demonstrates that this approach is size dependent.

We also observed that the second APTES based approach, in which the plane glass was immersed in mixture of APTES and Au NP solution the thickness and absorption value was tuned by changing the immersion time. Glass slides immersed for 15 hours, 20 hours and 24 hours had an increasing thickness, and increasing absorption values of 30%, 50% and 75% respectively. This technique is dependent in time as with increasing time the thickness of the layer can be increased. The reverse micelle approach used provides us with 2% absorption value which is an indicative of less material deposited on the surface which is not optimal for LSPR sensing. Looking at the wide width of all the a absorbance peaks it can be concluded that the particle size distribution on the surface is very broad reducing the sensitive of the

surface sensor. In order to increase the sensitivity it is also important to narrow down the size distribution of Au NP solutions used.

After optimizing all the procedures and establishing a protocol which could be used to fabricate sensors with specific and constant surface morphology observed under AFM, these images can be used to model this created Python tool and make an advanced quality control tool capable of distinguishing between AFM images of further fabricated sensor surfaces on the basis of their sensitivity. In order to create such a quality control tool we would require set AFM images of standard fabricated sensors to setup standard threshold values. Different parameters could be used to setup these standard thresholds including the height distribution, shape of height distribution histogram, average height and number of particles which lie above and below the average height. Later, the AFM images of the randomly fabricated sensors could be analyzed and values could be compared against the threshold values in an automated fashion to determine if the fabricated sensor falls within the standard range or not.

6. Conclusion

From this software development project we were successfully able to use Python to do image analysis of AFM images in an automated fashion. The developed program works well on images which have nanoparticles separated apart from each other and are not clustered. This program deals with some degree of clustering but heavier clusters add on some errors in analysis. This program also gives the height distribution of the nanoparticles. The average height achieved from this program still deviates a little from the average height achieved manually. However, this problem can be resolved by finding the average height from the list of heights in the biggest bin of height distribution histogram because that bin has the range of highest heights present on the image. I have confirmed and observed the pattern that the average of the biggest bin matches the manually calculated average height. This program has a potential to be used in quality control purposes with some optimization and standard data. There are also some limitations associated with this program including difficulties with differentiating particles from a cluster of particles, but this can be improved by using ideas as suggested in section 7 (next steps). From the UV-Vis data, we suggest that there is a presence of SPR in all the fabricated chips, but the quality of SPR present needs to be improved. This can be improved by achieving narrow size distribution and consistent closely packed structures of arranged nanoparticles. Additionally, we observe that either there is a very less SPR signal, which suggests very less amount of gold nanoparticles on the surface, or the SPR peak is very broad, which suggests the uncontrolled, and broader size distribution of nanoparticles on the surface. This overall project was a great learning experience and from recent outcomes, we can suggest that it can produce promising results with the suggested optimizations.

7. Next Steps

This tool can be applied in different places for quality control of different nano-engineerings like, nanoparticle synthesis fabrication, nano-surface fabrication. There is still a lot more to be improved in this program and can be done by making more sophisticated algorithms. Machine learning is a newly emerging field which can be applied to automate the first step of this procedure which is creating mask and overlap of mask plus original image. The limitation of this program is that when there is clustering of particles it cannot differentiate the particles within the cluster. There have been lot of deep learning algorithms used for counting and differentiating clusters in different areas like counting humans, counting bacterial colonies in a solid growth media. There are different models trained for these purposes and can be exploited to train machine with our own data sets. In Somaya A. Et al. (11) they demonstrated the use of preexisting deep learning (DL) algorithms to train a their machine from their small image data set of bacterial culture plates with colonies on it. They used the deep learning model used for counting objects in congested scenes into a specialized cell colony counting model (11). The well known neural network known as CSRNet is used in this application and it uses the density mapping to count number of entities. This network was previously used to count the humans in contested places but is also transferable to other areas which require counting. We use the similar model and use Transfer learning methods by using our data sets.

As you can see in the example figure 7.1 the areas marked with black are clusters of two or more particles together and because of these clusters this program cannot differentiate them, and sees them as one single entity. Because of this clustering and inability of software to differentiate leads to errors in counting and coordinate extraction. This can also be solved and software can be further optimized. A brief idea on how it can be handled is by finding the area of each particle in the image (this will also include the area of cluster). This recent program can be used successfully to find the area of each particle. This way we can find a range in which most of the areas lie and clusters will appear as outliers. For example if we have 100 particles in total, 96 of them are in range of 4 to 5 cm square and 4 are in range of 8 to 11 cm square. This distribution tells that those four are the outliers and are probable clusters. Now our goal is to find how many particles approximately lie in those clusters. This can be done by finding the average particle area lying within the range of maximum number of particles which is 96 particles in this example. This will give a average particle area for non-clustered particles. Using this average we can find how can particles approximately lie in a cluster. For example if we get an average of 4.8 cm square and we have a cluster of 11 cm square, if we divide 11 with 4.8 we can comment that there are approximately two particles in this cluster. After finding number of possible particles in each cluster we can divide the cluster into pieces by fitting the most feasible shape like a circle or hexagon which could divide the cluster into most representative manner.

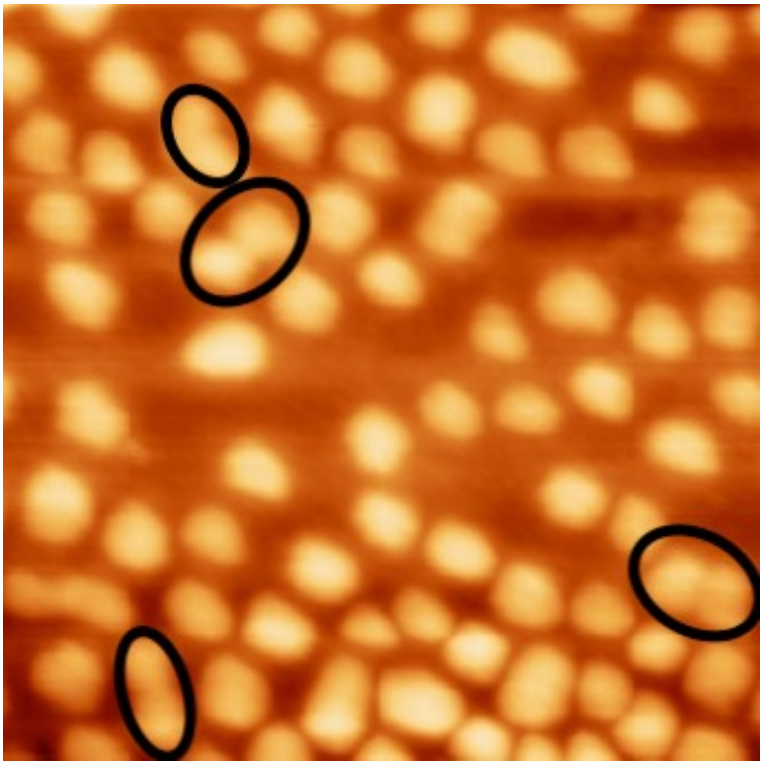

Figure 7.1 - Example Figure

For further optimization of the LSPR sensor surfaces fabrication using different approaches we can change following parameters:
For micelle based nanoparticles mediated fabrication, the problem we are encountering is that there is not enough gold on the surface to generate a detectable SPR signal. This can be improved by changing the spin coating speed. The benefit of using this technique is that the size of nanoparticles lies within a very narrow size distribution and can be very finely tuned for different sizes. Closely packed arrangement of nanoparticles can be achieved by reducing the spin coating speed and making the precise dropping of micelle solution, which can be achieved my making a precise fitting or a mechanical arrangement.

For the fabrication of LSPR sensors from APTES based adhesion of aqueous solution synthesized gold nanoparticles, we need to optimize more variables as compared to micelle based technique. But the benefit of this technique is that once optimized, it can be cheaper comparatively. In order to optimize this technique two things needs to be optimized which include a gold nanoparticle synthesis procedure to achieve a narrow size distribution and the second one is functionalizing APTES on a glass surface.

APTES functionalization is dependent on the number of available hydroxyl groups present on the surface. Notably, the number of hydroxyl groups that can be increased by oxidizing the surface by oxygen etching. Also, adhesion can be increased by increasing the number of

available amine groups present on the surface. This can be done by using vapour phase or alcoholic phase deposition of APTES on glass.

Aqueous phase synthesis of nanoparticles can be improved by changing a lot of different parameters and requires more deeper research in the field of synthesizing gold nanoparticles using tri-sodium citrate as a reducing agent.

The newly discovered technique, where gold nanoparticles are mixed with APTES solution and plain glass is immersed in it, gives us a layer of gold NPs on the surface. We also achieved layers of different thickness by changing the incubation time. This technique can also be used but has never been researched before as it needs more optimization. It can be optimized by changing parameters including the APTES concentration and incubation time.

8. References

1. Ghosh, S. K., Pal, T. (2007). Interparticle coupling effect on the surface plasmon resonance of gold nanoparticles: from theory to applications. Chemical reviews, 107(11), 4797–4862. https://doi.org/10.1021/cr0680282

2. Tokareva, I., Minko, S., Fendler, J. H., Hutter, E. (2004). Nanosensors based on responsive polymer brushes and gold nanoparticle enhanced transmission surface plasmon resonance spectroscopy. Journal of the American Chemical Society, 126(49), 15950–15951. https://doi.org/10.1021/ja044575y

3. Iyer, K. S.; Zdyrko, B.; Malz, H.; Pionteck, J.; Luzinov, I. Macromolecules 2003, 36, 6519-6526

4. Ruhe, J.; Ballauff, M.; Biesalski, M.; Dziezok, P.; Grohn, F.; Johannsmann, D.; Houbenov, N.; Hugenberg, N.; Konradi, R.; Minko, S.; Motornov, M.; Netz, R. R.; Schmidt, M.; Seidel, C.; Stamm, M.; Stephan, T.; Usov, D.; Zhang, H. AdV. Polym. Sci. 2004, 165, 79-150

5. Biesalski, M.; Johannsmann, D.; Ruhe, J. J. Chem. Phys. 2002, 117, 4988-4994

6. Houbenov, N.; Minko, S.; Stamm, M. Macromolecules 2003, 36, 5897-5901

7. Guo, X.; Ballauff, M. Phys. ReV. E 2001, 64, 051406

8. Shin YB, Lee JM, Park MR, et al. Analysis of recombinant protein expression using localized surface plasmon resonance (LSPR). Biosensors Bioelectronics. 2007 Apr;22(9-10):2301-2307. DOI: 10.1016/j.bios.2006.12.028

9. Xie, L., Yan, X., Du, Y. (2014). An aptamer based wall-less LSPR array chip for label-free and high throughput detection of biomolecules. Biosensors bioelectronics, 53, 58–64. https://doi.org/10.1016/j.bios.2013.09.031

10. Nicoya Lifescience, Gold Nanoparticles for Surface Plasmon Resonance

11. S. A. Albaradei et al., "Automated Counting of Colony Forming Units Using Deep Transfer Learning From a Model for Congested Scenes Analysis," in IEEE Access, vol. 8, pp. 164340-164346, 2020, doi: 10.1109/ACCESS.2020.3021656